MÄLARDALEN UNIVERSITY
SWEDEN

School of Education, Culture and Communication
Division of Mathematics and Physics

MASTER'S DEGREE PROJECT IN MATHEMATICS

Implied volatility with HJM–type Stochastic Volatility model

by

Thi Diu Cáp

MAA515 — Examensarbete i matematik för masterexamen

DIVISION OF MATHEMATICS AND PHYSICS
MÄLARDALEN UNIVERSITY
SE-721 23 VÄSTERÅS, SWEDEN

MÄLARDALEN UNIVERSITY
SWEDEN

School of Education, Culture and Communication
Division of Mathematics and Physics

MAA515 — Master's Degree Project in Mathematics

Date of presentation:
11^{th} June 2021

Project name:
Implied volatility with HJM–type Stochastic Volatility model

Author(s):
Thi Diu Cáp

Version:
17th June, 2021

Supervisor(s):
Ying Ni

Reviewer:
Jean-Paul Murara

Examiner:
Anatoliy Malyarenko

Comprising:
30 ECTS credits

Abstract

In this thesis, we propose a new and simple approach of extending the single-factor Heston stochastic volatility model to a more flexible one in solving option pricing problems. In this approach, the volatility process for the underlying asset dynamics depends on the time to maturity of the option. As this idea is inspired by the Heath–Jarrow–Morton framework which models the evolution of the full dynamics of forward rate curves for various maturities, we name this approach as the HJM–type stochastic volatility (HJM–SV) model. We conduct an empirical analysis by calibrating this model to real-market option data for underlying assets including an equity (ABB stock) and a market index (EURO STOXX 50), for two separated time spans from Jan 2017 to Dec 2017 (before the COVID–19 pandemic) and from Nov 2019 to Nov 2020 (after the start of COVID–19 pandemic). We investigate the optimal way of dividing the set of option maturities into three classes, namely, the short-maturity, middle-maturity, and long-maturity classes. We calibrate our HJM–SV model to the data in the following way, for each class a single-factor Heston stochastic volatility model is calibrated to the corresponding market data. We address the question that how well the new HJM–SV model captures the feature of implied volatility surface given by the market data.

Keywords: Implied volatility surface, stochastic volatility model, HJM framework

Acknowledgements

I thank my family for great support me to complete this master's thesis. I extend my gratitude to my supervisor Ying Ni for her professional guidance throughout the entire research process as well as her helpful suggestions and valuable helpful comments to me while I am writing the thesis.

Contents

Acronyms

ATM At The Money

BSM Black–Scholes–Merton

CIR Cox–Ingersoll–Ross

FFT Fast Fourier Transform

HJM Heath–Jarrow–Morton

HJM–SV Heath–Jarrow–Morton type Stochastic Volatility

ITM In The Money

IVS Implied Volatility Surface

LV Local Volatility

MSE Mean Square Error

OTM Out The Money

SDE Stochastic Differential Equations

SV Stochastic Volatility

List of Figures

List of Tables

1 Introduction

Advancements in technology are driving a transformation in finance. Assets trading can be easily done through various platforms and markets. Thus, trading is being done in an ever–increasing diverse set of assets and with financial contracts on just about anything whose value is changing in time. Everyone can be a market participant, and they must decide upon what they think such instruments are worth–to quote bid and/or ask values. However, there are a number of difficulties that market participants need to deal with. First, it is challenging to decide what a reasonable price for an intricate contract is. Various research works, e.g. [5, 17, 12, 3, 22], have been trying to eliminate certain level of subjective thinking and riskiness by attempting to price derivatives theoretically. By making assumptions on the dynamics of the markets and the actions of its participants, theoretical models have been developed to pricing financial derivatives. The most well–known and widely used is the Black–Scholes–Merton framework [5] in which the price processes must satisfy the Black–Scholes differential equation. Analytical price expressions for normal (vanilla) options can be found by solving the differential equation. Second, measuring the risk in the financial market is also difficult. Risk measures are major components in modern portfolio theory, which is a standard financial and academic methodology for assessing the performance of a stock or a stock fund as compared to its benchmark index.

Volatility has always been a central topic for measuring risk in the financial market. Volatility is a statistical measure of the dispersion of returns for a given security or market index. In most cases, the higher the volatility, the riskier the security. Volatility is often measured as either the standard deviation or variance between returns from same security or market index. An accurate estimation of volatility can contribute to good performances in speculation and hedging. The introduction of Implied Volatility Surface (IVS) is one of the methods to analyze volatility across options' strike prices and time to maturity. Thus, various models [5, 19, 13, 3, 4] of surface construction and its dynamics were developed and have been improved over time.

In particular, the Black–Scholes model and formula [5] were widely used after their proposal as a guiding tool for pricing vanilla options. However, after the 1987 stock market crash there are questions about the applicability of the Black–Scholes model. The 1987 global market crash made the market had become more afraid of unusual events and generally put a higher price on riskier derivatives than before. It also altered implied volatility patterns that arise in pricing financial options. It has been seen a magnification of phenomena where volatility surfaces for global indices have been characterized by the volatility smiles and skewes. J. Hull stated in his book [19] that

> "Equity options traded in American markets did not show a volatility smile before the crash but began showing one afterward."

So what are volatility smiles and skewes?. In the broad definition, volatility smiles and skewes are a measure of the failure of market prices for vanillas to exactly agree on the assumptions in the theoretical Black–Scholes framework. Thus, using the Black–Scholes formula for vanillas in reverse one can find a volatility value corresponding to each option. Such volatilities are called implied volatilities and when plotting them against the strike prices of the corresponding options, one can often see that the plot gives a convex set of data points–resembling a smile or a skew in shape, where the Black–Scholes formula predicts a constant.

Moreover, the volatility smiles and skewes terms can also be explained by the resulting graph when implied volatility is plotted against strike price. The graph is typically downward sloping for equity markets or valley-shaped for currency markets. For markets where the graph is downward sloping, such as for equity options, the term "volatility skew" is often used. For other markets, such as Foreign exchange options or equity index options, where the typical graph turns up at either end, the more familiar term "volatility smile" is used. For example, the implied volatility for upside (i.e. high strike) equity options is typically lower than for at the money equity options. However, the implied volatilities of options on foreign exchange contracts tend to rise in both the downside and upside directions. In equity markets, a small tilted smile is often observed near the money as a kink in the general downward sloping implicit volatility graph. Sometimes the term "smirk" is used to describe a skewed smile.

There exists numerous empirical studies that have pointed out that the volatility of the value of an underlying asset is not constant. Some early studies include Mandelbrot [25] and Officer [30], and more recent research works such as [13], [33]. Stochastic volatility modeling frameworks have come with attempts to correct this problem with Black Scholes by allowing volatility to fluctuate over time [2]. Some of well–known stochastic volatility models are Heston [17] , Stein and Stein [36], Melino and Turnbull [26], Hull and White model [19]. Several papers have documented that these stochastic volatility models are helpful in modeling the smirk, and that the modeling of the leverage effect is critical in this regard (e.g., see Bakshi, Cao, and Chen [3], Bates [4], Chernov and Ghysels[8], Jone [21], Nandi [28] and Pan [31]). Stochastic volatility models can also address term structure effects by modeling mean reversion in the variance dynamic. Consequently, many papers use a single–factor stochastic volatility model as the starting point for more complex models.

One of the most wide-used stochastic volatility models is Heston[17] as it provides a closed-form valuation formula that can be used to efficiently price plain vanilla options. One of the main limitations of this model is the presence of the parameters in the model which have to be calibrated carefully to provide a decent estimate of the option prices. Further, it is found that the model suffers when it comes to predicting the option prices for short-term options as the model fails to capture the high implied volatility. In short, the single-factor Heston model is not rich enough

to capture the structure of implied volatilities across maturities. As a remedy, various extensions to the Heston model have been proposed, for example, the Double Heston model by Christoffersen et. al [9] and the Gatheral model[14].

In this thesis, we propose a new extension of the single–factor Heston stochastic volatility model to a more flexible one in capturing the structure of the market implied volatility surface, i.e. the market implied volatility as a function of both strike prices and maturities. In this approach, the volatility process for the underlying asset dynamics depends on the time to maturity of the option. As this idea is inspired by the Heath–Jarrow–Morton framework which models the evolution of the full dynamics of forward rate curves for various maturities, we name this approach as the HJM–type stochastic volatility model, and hereafter shortened as the HJM–SV model. Using this HJM–SV model, there is one specific Cox–Ingersoll–Ross (CIR) volatility process for each time to maturity. Thus, not only the new model generates stochastic correlation between volatility and underlying derivative returns, but also expresses the dependence of volatility to the time to maturity of the derivative instruments.

Our model is a data-driven one, to evaluate the performance of this model, we use a large data set on daily implied volatility surfaces for two different underlying and two separate one-year-long time periods. We note that the COVID–19 pandemic has an obvious impact on the financial market and hence how underlying asset models work, our data sets, therefore, cover both the period before the pandemic and after the start of it. For each day, the implied volatility surface consists of implied volatilities for 130 options with 10 maturities and 13 strikes. At this stage of research, we study a simplified form of HJM–SV model, in which we group the 10 maturities into three classes. Our contribution is to calibrate this three-class HJM–SV model to the data sets and evaluate the performance of our model by experimental calibration studies.

Knowledge of the structure and dynamics of implied volatility is valuable for pricing options. Accomplishing the construction of a surface requires a relevant model to reproduce the options prices and carefully estimating parameters. The main contribution of this work is the construction of the implied volatility surface based on the pricing of ABB stock[15] and EURO STOXX 50 Index[20] derivatives under the assumption that the underlying follows the Heath–Jarrow–Morton (HJM)-inspired stochastic volatility with discontinuous jumps model, and the use of the Fast Fourier Transform (FFT) approach in calculating option premiums.

Our experimental results show that the HJM-inspired Stochastic Volatility (SV) without diffusion jump type model adequately fits observed short maturity option class (30 days) and medium maturity maturity option class (from 60 days up to 180 days) in period from Jan 2017 to Dec 2017 and from Nov 2019 to Nov 2020.

The remaining of the thesis is organized as follows. In Section 2, we introduce the theoretical background of different models of underlying asset prices, their volatil-

ity, and the Fourier based option pricing approaches. In particular, we focus on the SV model since it is closed to the author's proposed HJM–SV model. In Section 3, we describe the HJM–SV model and the data selection process. Section 4 demonstrates a calibration procedure with some highlighted techniques/algorithms used in the procedure. Parameter estimates and the implied volatility surfaces for the chosen sample data are shown in Section 4. The last section presents the author's conclusion and some potential research directions in the future. The thesis also includes appendices of examples to sample data used in calibration as well as some calibrated result tables.

2 Theoretical background

In this section, we present the concepts of financial derivative underlying asset prices and option pricing models. More specifically, those concepts cover the key dimensions of the problem at hand and also provide the fundamental to our proposed HJM–SV model. The Black–Scholes–Merton (BSM) model [5] and Heston model [17] are shortly recalled in this section in order to present the relative characteristic functions used in Fourier–based method of option pricing.

2.1 Models for the underlying asset

In mathematical finance, the asset S_t that underlies a financial derivative, is typically assumed to follow a stochastic differential equation of the form

$$dS_t = (r_t - q_t)S_t dt + \sqrt{V_t} S_t dW_t, \tag{1}$$

where r_t is the instantaneous risk free rate, giving an average local direction to the dynamics, q_t is the dividend yield rate, and W_t is a Wiener process, representing the inflow of randomness into the dynamics. The amplitude of this randomness is measured by the instant volatility V_t. In the simplest model i.e. the Black–Scholes model, V_t is assumed to be constant; in reality, the realized volatility of an underlying actually varies with time. When such volatility has a randomness of its own, which often described by a different equation driven by a different Wiener process, the model above is called a stochastic volatility model.

2.1.1 Local volatility model

When a stochastic volatility is merely a function of the current asset level and of time, we have a Local Volatility (LV) model. The LV model is a useful simplification of the stochastic volatility model.

"Local volatility" is thus a term used in quantitative finance to denote the set of diffusion coefficients, $V_t = V(S_t, t)$, that are consistent with market prices for all options on a given underlying. This model is used to calculate exotic option valuations which are consistent with observed prices of vanilla options.

2.1.2 Discontinuous jump models

In contrast to basic insights into continuous-time asset-pricing models that have been driven by stochastic diffusion processes with continuous sample paths, jump diffusion processes have been used in finance to capture discontinuous behavior in asset pricing. As described in [27], the validity of Black–Scholes formula depends on whether the stock price dynamics can be described by a continuous-time diffusion process whose sample path is continuous with probability 1. Thus, if the stock price dynamics cannot be represented by stochastic process with a continuous sample path, the Black–Scholes solution is not valid. In other words, as the price processes feature big jumps, i.e. not continuous, continuous-time models cannot explain why the jumps occur, and hence not adequate. In addition, Ahn and Thompson [1] also examined the effect of regulatory risks on the valuation of public utilities and found that those "jump risks" were priced even though they were uncorrelated with market factors. It shows that jump risks cannot be ignored in the pricing of assets. Thus, a "jump" stochastic process defined in continuous time, and also called as "jump diffusion model" was rapidly developed.

The jump diffusion process is based on Poisson process, which can be used for modeling systematic jumps caused by surprise effect. Suppose we observe a stochastic process St, which satisfies the following stochastic differential equation with jump.

$$dS_t = (r - r_J)S_t dt + \sqrt{V}S_t dZ_t + J_t S_t dN_t,$$

where r is the constant short rate, V the constant volatility, Z_t a standard Brownian motion, N_t a Poisson process with intensity λ. Furthermore, J_t is the jump at date t with the distribution $\log(1 + J_t) = \boldsymbol{N}\big(\log(1 + \mu_J) - \frac{\delta^2}{2}, \delta^2\big)$, where $\boldsymbol{N}$ is the cumulative distribution function of a standardized normal random variable.

Finally, $r_J = \lambda(e^{\mu_J + \delta^2/2} - 1)$.

2.1.3 Stochastic volatility model

Heston model [17] is the well–known pricing models of European options with SV. The Heston model assumes that the underlying stock price, S_t, follows a BSM–type stochastic process, while the variance V_t also follows a stochastic process presented by the CIR model [10]. In their original paper, the CIR process is given by:

$$a(b - r_t)dt + \sigma\sqrt{r_t}dW_t, \tag{2}$$

where W_t is a Wiener process which modelling the random market risk factor, and a, b, σ are the parameters. The parameter a corresponds to the speed of adjustment to the mean b, and σ corresponds to volatility.

Following the mathematical formulation of CIR given by (2), the stock price and its variance in Heston model, are driven by the following system of Stochastic

Differential Equations (SDE):

$$dS_t = (r - q)S_t dt + \sqrt{V_t} S_t dW_{1,t}$$

$$dV_t = \kappa(\theta - V_t)dt + \sigma\sqrt{V_t} dW_{2,t}$$

where $E[dW_{1,t}, dW_{2,t}] = \rho dt$, and the parameter of the model are: W_t is Brownian motion; r is the drift of the process of the stock in the martingale measure; q is the rate of paying dividends; $\kappa > 0$, $\theta > 0$, $\sigma > 0$ are respectively, the mean reversion speed, the mean reversion level, the volatility of the variance; and $V_0 > 0$ is the initial (time zero) level of the variance.

The parameter κ controls the speed of mean reversion of the volatility, σ is the volatility of the volatility, and θ is the long-term of the variance process. An important feature of the Heston model is the stochastic volatility which allows to reproduce the implied volatility smile present in many financial markets. Each parameter has a specific effect on the implied volatility curve generated by the dynamics so it is interesting to study uncertainty quantification for the implied volatility as well as for the prices of certain financial products [37].

If $2\kappa\theta > \sigma^2$, so-called Feller condition, is satisfied and the positivity of V_t is guaranteed, otherwise it may reach zero. The Feller condition is difficult to satisfy in practice, so in this work the cases with and without Feller conditions will be considered.

2.1.4 Combined models

The three model types, which are LV, SV, and discontinuous jump processes, can be combined to more complex and far–reaching models. One motivation for such combining is that stochastic volatility models tend to underestimate smile convexity at short maturities and jump–diffusion models as well as local volatility models tend to underestimate smile convexity at long maturities. When being combined, they help with each others shortcomings. In [35], the authors claim that stochastic volatility–jump diffusion models matches the market better than the use one of the three types alone.

2.2 Option valuation method

In the recent years, Fourier based option pricing approaches is well–known as an efficient method for valuing financial derivatives because it satisfies the important demands of being fast and accurate. Moreover, this option pricing approach allows the use of semi–analytic valuation formulas for European options whenever the characteristic function of the stochastic process representing the underlying is known [18]. We believe that applying Fourier–based method allows us to efficiently calculate the model price and calibrate the parameters to SV type model in different

designed markets.

Definition 1. (Fourier Transform). Given an integrable function $f(x)$, its *Fourier transform* is defined as the function [18]:

$$\hat{f}(u) \stackrel{\text{def}}{=} \int_{-\infty}^{\infty} e^{iux} f(x) dx, \tag{3}$$

with u either real or complex, e^{iux} is called the phase factor.

The *Fourier inverse transform* allows to recover $f(x)$ via the integrals [18]:

$$f(x) = \frac{1}{2\pi} \int_{-\infty}^{\infty} e^{-iux} \hat{f}(u) du, \text{ for } u \in \mathbb{R} \tag{4}$$

$$f(x) = \frac{1}{2\pi} \int_{-\infty+iu_i}^{\infty+iu_i} e^{-iux} \hat{f}(u) du, \text{ for } u \in \mathbb{C} \text{ with } u = u_r + iu_i \tag{5}$$

Parseval's Relation. Given two square–integrable functions f, g taking values in $\mathbb{C}$, the following relation holds:

$$\langle f, g \rangle = \frac{1}{2\pi} \langle \hat{f}, \hat{g} \rangle \tag{6}$$

with $\langle \cdot, \cdot \rangle$ denoting the inner product between the two argument functions: $\langle f, g \rangle \stackrel{\text{def}}{=} \int_{-\infty}^{\infty} f(x) \overline{g(x)} dx$.

Definition 2. (Characteristic Function) The characteristic function $\hat{q}$ of a random variable X is the Fourier transform of its probability density function $q(x)$ [18],

$$\begin{aligned} \hat{q}(u) &\stackrel{\text{def}}{=} \int_{-\infty}^{\infty} e^{iux} q(x) dx \\ &= E^Q(e^{iuX}), \end{aligned} \tag{7}$$

where the superscript E^Q refers to expectation under probability measure Q with probability density function $q(x)$.

2.3 No–Arbitrage Option Pricing

We consider an economy over a fixed time interval $[0, T] \in R^+$. At date 0 there is uncertainty about the true state of the economy at the terminal date T. The set of possible states, however, is known. The set of all possible states ω is denoted by Ω and called the state space. Subsets of Ω are called events. The family of sets that forms the set of observable events is an algebra in Ω.

Let's consider a *discrete market model* where, for a fixed time interval $[0, T]$, we suppose that all transactions take place only at times

$$0 = t_0 < t_1 < \cdots < t_N = T.$$

The market consists of one riskless asset (bond) B with unitary face value, such that $B_t = e^{-r(T-t)}$; and d risky assets $S = (S_1, S_2, \cdots, S_d)$ that are stochastic processes defined on a discrete probability space $(\Omega, \mathcal{F}, P)$. We assume Ω has a finite number of elements, $\mathcal{F} = P(\Omega)$ and $P(\omega) > 0$ for any $\omega \in \Omega$.

In a discrete-time market, on a discrete probability space $(\Omega, \mathcal{F}, P)$ the following theorems hold [32]:

Theorem 1. (The First Fundamental Theorem of Asset Pricing) The discrete market is arbitrage free if, and only if, there exists at least one risk neutral probability measure that is equivalent to the original probability measure, P.

Theorem 2. (The Second Fundamental Theorem of Asset Pricing) An arbitrage–free market (S_t, B_t) consisting of a collection of stocks S and a risk–free bond B is complete if and only if there exists a unique risk–neutral measure that is equivalent to P and has numeraire B_t.

Let's consider a *continuous market model* $\mathcal{M} = \{(\Omega, \mathcal{F}, \mathbb{F}, P), T, (S, B)\}$, where:

- $(\Omega, \mathcal{F}, \mathbb{F}, P)$ is a probability space with a filtration $\mathbb{F}$ of non-decreasing sigma-algebras,
- $T \in (0, \infty)$ is the final date,
- (S, B) is the set of tradable assets: a positive stock index S_t, where $t \in [0, T]$ which is a semimartingale and a risk–less bond B with unitary face value, such that $B_t = e^{-r(T-t)}$, with short rate $r \geq 0$.

By the Fundamental Theorem of Asset Pricing, if we assume no free lunch with vanishing risk, then there exists a P–equivalent martingale measure Q under which all stochastic processes of the market model are martingales. The value at time t of an European option maturing at T is then obtained by discounting its expected payoff under the equivalent martingale measure Q. Therefore, the price of a European call option is:

$$C_t = e^{-r(T-t)} E_t^Q(C_T) \quad \text{with } C_T = (S_T - K)^+ \text{ and } K > 0 \tag{8}$$

When we move to the integral representation we have:

$$C_t = e^{-r(T-t)} \int_0^\infty C_T(s) Q(ds) = e^{-r(T-t)} \int_0^\infty C_T(s) q(s) ds \tag{9}$$

Problems arise when the risk–neutral probability density function $q(s)$ of S_T is not known, as it quite often happens. However, whenever the characteristic function of S_T is known it can be used along with the Fourier transform of the option's payoff in order to determine the option price, and this sets the base for Fourier–based pricing.

2.4 Fourier–based Option Pricing

Using the mathematical tools provided in the previous sections, Fourier–based pricing approaches were developed in order to obtain a more general valuation of option prices, where the fundamental ingredient is the characteristic function of the underlying stochastic process. Furthermore, this kind of pricing proves to be accurate and efficient: numerical evaluation methods reach high levels of accuracy while maintaining low computational costs and high speed. We review several essential concepts on Fourier Series and Fast Fourier Transform in this section and our discussion is based on [18].

2.4.1 Lewis Approach

Lemma 1. (Call Option Transform) [18]. We consider a European call option with payoff $C_T \stackrel{\text{def}}{=} (e^s - L)^+$, with $s \stackrel{\text{def}}{=} \log S$. The *Fourier transform* of C_T is

$$\hat{C}_T(u) = -\frac{K^{iu+1}}{u^2 - iu}, \tag{10}$$

for $u = u_r + iu_i$, with $u_i > 1$.

The proof to Lemma 1 is provided in [18].

We can now retrieve the payoff function $C_T(s)$ via Fourier inversion, obtaining the following expression:

$$C_T(s) = \frac{1}{2\pi} \int_{-\infty+iu_i}^{\infty+iu_i} e^{-ius} \hat{C}_T(u) du \tag{11}$$

The value of the call option in $t = 0$ is then obtained by applying martingale pricing. Discounting the expected payoff as in (8) and using the transform representation of C_T yields:

$$\begin{aligned} C_0 &= e^{-rT} E_0^Q(C_T) \\ &= e^{-rT} E_0^Q \left(\frac{1}{2\pi} \int_{-\infty+iu_i}^{\infty+iu_i} e^{-ius} \hat{C}_T(u) du \right) \\ &= \frac{e^{-rT}}{2\pi} \int_{-\infty+iu_i}^{\infty+iu_i} E_0^Q(e^{i(-u)s}) \hat{C}_T(u) du \end{aligned} \tag{12}$$

where we have assumed that the interchange of integration and expectation is valid. We derive an application of Parseval's relation to the risk–neutral pricing equation.

Recall that by equation (7), when replacing u by $-u$, we have:

$$\begin{aligned} \hat{q}(-u) &\stackrel{\text{def}}{=} \int_{-\infty}^{\infty} e^{i(-u)x} q(x) dx \\ &= E^Q(e^{i(-u)X}), \end{aligned} \tag{13}$$

From (12) and (13), we obtain the call option price at time $t = 0$ as the following:

$$C_0 = \frac{e^{-rT}}{2\pi} \int_{-\infty+iu_i}^{\infty+iu_i} \hat{q}(-u)\hat{C}_T(u)du$$

Further computations are done assuming $S_t \overset{\text{def}}{=} S_0 e^{rt+X_t}$ with X_t a Lévy process, namely an adapted real valued process with $X_0 = 0$ and stationary independent increments.

Then, being $\phi(\cdot)$ the characteristic function of X_T we can write $\hat{q}(-u) = e^{-iuy}\phi(-u)$, with $y = \log S_0 + rT$. We define $k = \log(S_0/K) + rT$, and substitute all quantities in the option's value expression, obtaining:

$$C_0 = -\frac{Ke^{-rT}}{2\pi} \int_{-\infty+iu_i}^{\infty+iu_i} e^{-iuk}\phi(-u)\frac{du}{u^2 - ui} \tag{14}$$

A pricing formula for the European call option can now be derived:

Proposition 1. [23]. Assuming $u_i \in (0, 1)$, the present value of a European call option is

$$C_0 = S_0 - \frac{Ke^{-rT}}{2\pi} \int_{-\infty+iu_i}^{\infty+iu_i} e^{-iuk}\phi(-u)\frac{du}{u^2 - ui} \tag{15}$$

When $u_i = 0.5$, the option is evaluated as

$$C_0 = S_0 - \frac{\sqrt{S_0 K}e^{-rT/2}}{\pi} \int_0^{\infty} \mathbf{Re}[e^{izk}\phi(z - i/2)]\frac{dz}{z^2 + 1/4} \tag{16}$$

The proof to proposition 1 is provided in [18].

Option pricing with Fourier–based methods can be implemented using direct integration methods. In alternative, we can use the Discrete Fourier Transform computed via the FFT.

2.4.2 Fourier Series and Discrete Fourier Transform

Definition 3. (Fourier series). A Fourier series to a 2π–periodic function f(x) is an infinite sum of the form:

$$f(x) = a_0 + \sum_{n=1}^{\infty}(a_n \cos nx + b_n \sin nx)$$

For an arbitrary interval $[-L, L]$, the Fourier series is

$$f(x) = a_0 + \sum_{n=1}^{\infty}\left(a_n \cos\left(\frac{n\pi}{L}x\right) + b_n \sin\left(\frac{n\pi}{L}x\right)\right)$$

with coefficients

$$a_0 = \frac{1}{2L}\int_{-L}^{L} f(x)dx$$
$$a_n = \frac{1}{L}\int_{-L}^{L} f(x)\cos\left(\frac{n\pi}{L}x\right)dx$$
$$b_n = \frac{1}{L}\int_{-L}^{L} f(x)\sin\left(\frac{n\pi}{L}x\right)dx$$

If $u \in \mathbb{C}$ with $u = u_r + iu_i$, Euler identity holds:

$$e^{iux} = e^{u_r x}(\cos(u_i x) + i\sin(u_i x))$$

so that the function $f(x)$ can be written as

$$f(x) = \sum_{n=-\infty}^{\infty} c_n e^{i\frac{n\pi}{L}x} \tag{17}$$
$$c_n = \frac{1}{2L}\int_{-L}^{L} f(x)e^{-i\frac{n\pi}{L}x}dx \tag{18}$$

What we get is a complex Fourier series from which we can obtain a Fourier transform representation in discrete form.
Setting $k_n = \frac{2\pi}{L}$, $\hat{c}(k_n) = c_n$ and Δ such that $\Delta n = 1$ and $\frac{L}{\pi}\Delta\frac{2\pi}{L} = 1$ yelds

$$f(x) = \frac{L}{\pi}\sum_{n=-\infty}^{\infty} \hat{c}(k_n)e^{ik_n x}\Delta k_n$$

We now define $\hat{f}(k_n) = \frac{L}{\pi}\hat{c}(k_n)$, so that

$$f(x) = \sum_{n=-\infty}^{\infty} \hat{f}(k_n)e^{ik_n x}\Delta k_n$$

and

$$\hat{f}(k_n) = \frac{L}{\pi}\frac{1}{2L}\int_{-L}^{L} f(x)e^{-ik_n x}dx$$

Taking the limit $L \to \infty$ the sum becomes an integral and we can drop the n subscript. Additionally, we change the sign in the phase factor and multiply $f(x)$ by 2π, retrieving the Fourier transform and inverse transform presented in (3) - (4)

$$\hat{f}(k) = \int_{-\infty}^{\infty} e^{ikx}f(x)dx$$
$$f(x) = \frac{1}{2\pi}\int_{-\infty}^{\infty} e^{-ikx}\hat{f}(k)dk$$

2.4.3 Fast Fourier Transform

FFT is an algorithm that computes the Discrete Fourier Transform. It consists in computing the following sums:

$$FFT(u) = \sum_{j=1}^{N} e^{-i\frac{2\pi}{N}(j-1)(u-1)} x(j), \quad u = 1, ..., N \tag{19}$$

Imposing the following relations:

$$v_j = v_1 + \eta(j-1), \text{ with } j = 1, ..., N$$

$$k_u = -b + \epsilon(u-1), \text{ with } u = 1, ..., N$$
$$\eta\epsilon = \frac{2\pi}{N}$$

where ϵ denote a regular spacing parameter. We have that the FFT returns N values for log-strikes k_u ranging from $-b$ to b with $b = 0.5N\epsilon$.
The integral in the expression for call option price (13) can be discretized in the following way:

$$\sum_{j=1}^{N} e^{-iv_j k_u} \frac{\phi(-v_j - i/2)}{v_j^2 + 1/4} \eta$$

Substituting v_j and k_u yields:

$$\sum_{j=1}^{N} e^{-i\eta\epsilon(j-1)(u-1)} e^{-i(v_1 k_u + k_1 \eta(j-1))} \frac{\phi(-v_j - i/2)}{v_j^2 + 1/4} \eta$$

We then introduce weights according to Simpson's rule:

$$\sum_{j=1}^{N} e^{-i\eta\epsilon(j-1)(u-1)} e^{-i(v_1 k_u + k_1 \eta(j-1))} \frac{\phi(-v_j - i/2)}{v_j^2 + 1/4} \frac{\eta}{3} (3 + (-1)^j - \diamond_{j-1}),$$

where $\diamond_n$ is the Kronecker delta function which takes value one for $n = 0$ and zero otherwise.
Finally, observing that $e^{-i\eta\epsilon(j-1)(u-1)} = e^{-i\frac{2\pi}{N}(j-1)(u-1)}$, we can directly use FFT to compute the expression above and retrieve the call option price [22].

2.5 Implied volatility and computing approach

As we stated in the introduction part, the Black–Scholes model was, and still, favourable used by investors for calculating the option premiums. The reason, perhaps, is thanks to its simplicity. Of all the variables used in the Black–Scholes model, the only one that is not known with certainty is volatility. At the time of pricing, strike price, time to maturity, current underlying asset price, interest rate and dividend yield, are clear and known. For this reason, in some literature, the

call prices for a vanilla option is simply express by $C = BS(\sigma)$. Theoretically, the implied volatility for a vanilla call option with price C can always be found from the inverse Black–Scholes formula. This is done by inputting the price C, strike price K, time to maturity T, current price of the underlying asset $S0$, interest rate r and dividend yield q in the formula $C = BS(S_0, K, T, r, q, \sigma)$. However, there is no closed-form inverse for it, but because it has a closed-form ν (volatility derivative) and the derivative is nonnegative, we can use the Newton–Raphson with a confidence level.

One can choose a starting value σ_0, for example, the authors of [6] provided a closed form estimate of implied volatility as follows:

$$\sigma = \sqrt{\frac{2\pi}{T}}\frac{C}{S_0} \tag{20}$$

If one uses (20) to compute the initial guess σ_0, then iterate:

$$\sigma_{n+1} = \sigma_n - \frac{BS(\sigma_n) - C}{\nu(\sigma_n)} \tag{21}$$

until reaching a solution of sufficient accuracy. This technique is known as Newton–Raphson method, which is a way to quickly find a good approximation for the root of a real–valued function $f(x) = 0$. The ν in the function (21) is one of the Greeks. By definition, the ν of an option is the sensitivity of the option price to a change in volatility. Black–Scholes formula for ν is:

$$\nu = S\sqrt{\frac{T}{2\pi}}e^{-\left(\log(\frac{S}{K})+(r+\frac{\sigma^2}{2})T\right)^2/(2\sigma^2 T)}$$

or, in the Black–Scholes d_1 notation,

$$\nu = S\sqrt{T}\phi(d_1), \quad \phi(\cdot) \text{ is the normal density}$$

A volatility smile or skew is a common graph shape that results from plotting the strike price and implied volatility of a group of options with the same underlying asset and expiration date. If the Black–Scholes model were completely correct, then the implied volatility for different strike prices should be a constant. In practice, this is unfortunately not the case. The implied volatility actually varies over time because the assumptions of the Black–Scholes model obviously are not always true. For instance, options with lower strike prices tend to have higher implied volatilities than those with higher strike prices. For a given strike price, implied volatility can be increasing or decreasing with time to maturity, giving rise to a shape known as a volatility smile because it looks like a person smiling. Volatility smiles are created by implied volatility changing as the underlying asset moves more In The Money (ITM) or Out The Money (OTM). Figure 1 shows that the more an option is ITM or OTM, the greater its implied volatility becomes. Implied volatility tends to be lowest with At The Money (ATM) options.

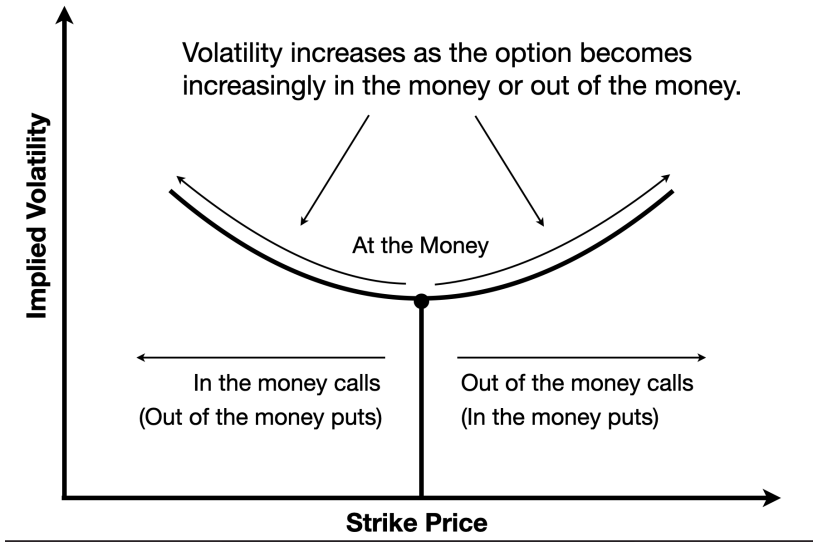

Figure 1: Volatility smiles.

3 Model implementation

In this section, we first motivate the idea of HJM–SV model for option pricing. Then, we describe our proposed model by SDEs. We implement and test the HJM–SV model using data on European call options on ABB stock and EURO STOXX 50 index options. The section also presents the choice of calibrating functional and selection of numerical optimization algorithms.

3.1 The HJM–SV model

The HJM framework is a general framework to model the evolution of interest rate curves – instantaneous forward rate curves in particular (as opposed to simple forward rates)[16]. Simple interest models before HJM framework present the short interest rate $r(t)$ as the only explanatory variable for entire money market, which seems unreasonable from an economic point of view. The method proposed by Heath–Jarrow–Morton uses the entire forward rate curve as their infinite dimensional state variable. Mathematical formulation for the instantaneous forward rate is $f(t,T)$, where $t \leq T$, and $f(t,T)$ is defined as the continuous compounding rate available at time T as seen from time t. Modeling the interest-rate evolution through the instantaneous short rate has some advantages, mostly the freedom one has in choosing the related dynamics [7]. Take one-factor interest rate models, for example, one is free to choose the drift and instantaneous volatility coefficient in the related diffusion dynamics as his own suitable consideration, with no general restrictions. Therefore, we would like to develop a model which can capture the evaluation of volatility for underlying asset price depending of the time to maturity of the derivative instrument. We start with the idea of HJM–SV model, in which there is one specific CIR process [10] presenting the underlying assets volatility process depending on time to maturity option. Based on the mathematical formulation

of CIR given by (2), we illustrate the model by the following SDE under risk–neutral probability.

$$dV_t^{T_i} \quad = \quad CIR^{T_i}(\kappa_i, \theta_i, \rho_i, \sigma_i, V_0^{T_i}) = \kappa_i(\theta_i - V_t^{T_i})dt + \sigma_i\sqrt{V_t^{T_i}}dB_{i,t}$$

where T_i denote the time to maturity for the ith option class, for i = 1, 2,... , N with an assumption that $T_1 < T_2 < ... < T_N$. Vector $(\kappa_i, \theta_i, \rho_i, \sigma_i, V_0^{T_i})$ is the parameter vector of CIR model for stochastic volatility $V_t^{T_i}$. Denote by Θ the parameter vector in the new model, thus we have

$$\Theta = (\kappa_i, \theta_i, \rho_i, \sigma_i, V_0^{T_i}) \tag{22}$$

- κ_i is the mean reversion speed
- θ_i is the mean reversion level
- σ_i is the volatility of the asset's volatility
- ρ_i is the correlation coefficient between the Wiener process (dW_t) in the SDE of underlying asset price and the Wiener process (dB_t) in the SDE of underlying asset's volatility, generally $E[dW_t, dB_{i,t}] = \rho_i dt$
- $V_0^{T_i}$ is the initial (time zero) level of the volatility.

In mathematical finance, mean reversion is a term for the assumption that an asset's price will tend to converge to the average price over the long–run time.

Besides, it is worth to mention that the main challenge in the HJM model is that all model parameters must be recalibrated at each point in time; there is no mechanism for sequential updating. Also, it is difficult to calibrate the model to actively traded prices in the market [34]. Thus, in the scope of the thesis work, we aim to demonstrate the HJM model with 3 maturity option classes, which includes short, medium and long time to maturity. Denote by T_1 the short time to maturity and T_2, T_3, respectively for the medium and long time to maturity. Moreover, the dynamic of the underlying asset price S is given by $dS = rSdt + \sqrt{V_t^T}SdW_t$. Then we have our initial proposed model for the simple case of 3 class time to maturity as the following:

$$\begin{cases} dS = rSdt + \sqrt{V_t^T}SdW_{1,t} \\ dV_t^{T_1} = CIR^{T_1}(\kappa_1, \theta_1, \rho_1, \sigma_1, V_0^{T_1}) \\ dV_t^{T_2} = CIR^{T_2}(\kappa_2, \theta_2, \rho_2, \sigma_2, V_0^{T_2}) \\ dV_t^{T_3} = CIR^{T_3}(\kappa_3, \theta_3, \rho_3, \sigma_3, V_0^{T_3}) \end{cases} \tag{23}$$

We aim to investigating whether the new HJM–SV model, given by (23) captures the market implied volatility surface better than other multi-factor models. In particular, we want to see if it outperforms or comparable the double Heston model in the paper [9].

Characteristic function In order to apply the Fast Fourier method for option valuation in the HJM–SV model we need to drive its characteristic function of underlying asset in the model. Fortunately, since we treat each time to maturity class separately with each other, i.e there is no correlation between $dB_{i,t}$, each time to maturity SV process is one CIR process. Based on the characteristic function of stock price in Heston model, [17], in which the characteristic function of stock price is also followed one CIR process, we can derive the characteristic function for stock price in HJM–SV as following:

$$\varphi_0^{(HJMSV(T_j))}(u, T_j) = \exp\left(A_1(u, T_j) + A_2(u, T_j)v_0\right) \tag{24}$$

where:

$$\begin{aligned}
c_1 &= \kappa_j \theta_j \\
c_2 &= -\sqrt{(\rho\sigma_i ui - \kappa_j)^2 - \sigma_j^2(-ui - u^2)} \\
c_3 &= \frac{\kappa_j - \rho\sigma_j uj + c_2}{\kappa_j - \rho\sigma_j ui - c_2} \\
A_1(u, T_j) &= r_{0,T} uiT + \frac{c_1}{\sigma_j^2}\Big\{(\kappa_j - \rho\sigma_j ui + c_2)T - 2log\Big[(\frac{1 - c_3 e^{c_2 T}}{1 - c_3}\Big]\Big\} \\
A_2(u, T_j) &= \frac{\kappa_j - \rho\sigma_j ui + c_2}{\sigma_j^2}\Big[\frac{1 - e^{c_2 T}}{1 - c_3 e^{c_2 T}}\Big],
\end{aligned}$$

and $\varphi_0^{(HJMSV(T_j))}(u, T_j)$ is the characteristic function of stock price with to time to maturity option class T_j, j = 1, 2, 3, in equation (23).

3.2 Data selection

We select the European call options data on ABB stock and EURO STOXX 50 index (SX5E) options for evaluating our the HJM–SV model. ABB stock is issued by ABB Ltd [15], a manufactures and sells electrification, industrial automation, and robotics and motion products for customers in utilities, industry and transport, and infrastructure worldwide. The SX5E [20] is a leading index of Europe's blue chip companies owned by the Deutsche Borse, Dow Jones and SWX Group. Similar to the Dow Jones 30 index in the U.S., the SX5E is made up of 50 of the largest and most liquid stocks across 12 eurozone countries. As of August 2020, the index is dominated by France (representing 36.4% of all total assets) and Germany (35.2%). The index futures and options on the SX5E, traded on Eurex, are among the most liquid products in Europe and the world. The SX5E is one of the most liquid indices for the Eurozone, thus it is an ideal underlying for financial products or for benchmarking purposes.

Our data on daily implied volatility surfaces is processed from the data product IvyDB Europe provided by OptionMetrics [24]. These implied volatility surfaces are constructed and interpolated using call options traded in Nasdaq OMX Nordic

Exchange (for ABB stock) and in Eurex (for EURO STOCXX 50 index). The time spans for the dataset are Jan 2017–Dec 2017 and Dec 2019–Dec 2020. In total, there are 523 days of implied volatility surfaces for ABB stock and 529 days for Euro Stoxx 50. For each trading day, we have a volatility surface for the two underlying assets. There are in total 10 maturities ranging from 30 to 730 calendar days. There are 13 implied strikes prices corresponding to the following values of Deltas (an quantity in the Black–Scholes option pricing formula): $0.20 + 0.05i, i = 0, 1, 12$. Hene, for each trading day, the constructed implied volatility surface are based on $N = 10 \times 13 = 130$ options.

Some remarks on the IvyDB Europe option pricing methodology [24]:

- For a given option, the appropriate interest rate input corresponds to the zero-coupon rate that has a maturity equal to the option's expiration, and is obtained by linearly interpolating between the two closest zero-coupon rates on the zero curve. Options with expiration greater than longest available maturity use the longest available maturity point.

- An assumption on that the security's current dividend yield (defined as the most recently announced dividend payment divided by the most recent closing price for the security) remains constant over the remaining term of the option. This "constant dividend yield" assumption is consistent with most dividend-based equity pricing models (such as the Gordon growth model) under the additional assumptions of constant average security return and a constant earnings growth rate.

- For dividend-paying indices, IvyDB Europe assumes that the security pays dividends continuously, according to a continuously-compounded dividend yield. The dividend yield for European indices is calculated based on linearized put-call parity. The present value of the dividend payments is:

  $$PV(div) = P - C + (S - K) + K(e^{rT} - 1)$$

  where r is interest rate to the option expiration and T is time to maturity in years. Then the implied dividend yield, q, is: $q = \frac{PV}{T-S}$

When selecting data for calibration, an approach similar to the one of Galluccio and Le Cam [12], who proposed to use at least three different options per maturity, we use a set of market quotes for European call options on ABB stock and SX5E as follows:

- Maturities: three maturities classes which corresponding to the short, medium and long maturity.

- strikes: 13 strikes per maturity in the initial calibration round and 8 strikes per maturity in the second calibration round. The differences between two round of calibration are objective function and the percentage of ITM and OTM options in the data.

- zero short interest rate for ABB stock and SX5E
- zero dividend yield rate for ABB stock and for SX5E.

To divide data selection into three maturity classes, we use:

- the short maturity option class, $T_1 = 30$ days
- the medium maturity option class 30 days $< T_2 \leq 182$ days
- the long maturity option class 182 days $< T_3 \leq 730$ days

Regarding our setting of a zero short interest rate and a zero dividend yield rate in the implementation, it will, in one hand, certainly simplify the calibration process and in the other hand, will affect the calibrating results as the interest rate and dividend yield are different for the market data and for the model. Therefore, instead of using the market options premium in the original data, we convert the option premiums from the market implied volatility. By doing so, we are using the same interest rate and dividend yield for both the market data and for the model, which creates a fair investigation on if the model captures well the implied volatility surfaces.

In addition, in the time span from Nov 2019 to Nov 2020, the stock market has experienced an extraordinary fluctuation. Thus we also would like to involve some investigation on how the implied volatility had behaved during that period. This lead us to divide data sample into two sub-data sets, before and after the stock market cash in March 2020.

March 2020 saw one of the most dramatic stock market crashes in history. In barely four trading days, Dow Jones Industrial Average plunged 6,400 points, an equivalent of roughly 26%. This crash was caused by the COVID–19 pandemic. The European countries economy also was affected strongly with a plunged in SX5E by nearly 37% in March 2020. As shown in Figure 2a and 2b, both the SX5E index and ABB stock experienced a significant drop in prices from the end of Feb 2020. In the appendix A.3 we include the evidence on CBOE Volatility Index (VIX) fluctuation between Nov 2019–Nov 2020, see Figure 14, to give a better explanation why March 2020 could be accepted as the borderline of the stock market before and after COVID–19. The VIX index is a real-time index that represents the market's and according to Figure 14 the index volatile up to 250% during first few days starting of March 2020.

Data used in Figure 2a, 2b, and 14 are taken from Yahoo Finance [11], the original currency of ABB and VIX index is in USD while SX5E index is in EURO, thus the author use average exchange rate USD-SEK between November 2020 and 9 May 2021 to convert the ABB stock price to its original price, in SEK.

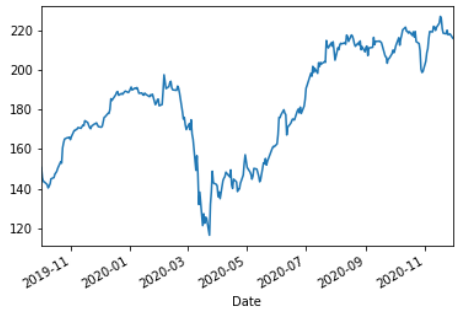

(a) ABB stock price from Jan 01, 2019 to Nov 30, 2020.

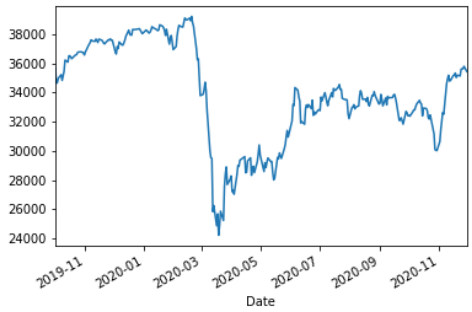

(b) SX5E index from Jan 01, 2019 to Nov 30, 2020.

Figure 2: ABB stock price and SX5E index from Jan 01, 2019 to Nov 30, 2020. Currency in SEK.

4 Calibration procedure and Results

In this section, we first present the objective function used in calibration process in the consideration to three most commonly functions used in literature. Afterward, we explain an useful technique, called Brute–Force algorithm, applying to estimate the HJM–SV model parameters by minimizing the objective function value. Finally, we present experiment results of the model on real data.

4.1 Objective function

To calibrate a financial market model, one needs a performance yardstick for the quality of the calibration–formally, an objective or error function which is to be minimized. Three objective functions most commonly used in the literature are:

- The Mean Square Error (MSE) of the price differences in currency units:

$$MSE = \min_{\Theta} \frac{1}{N} \sum_{n=1}^{N} (C_n^{market} - C_n^{model}(\Theta))^2 \tag{25}$$

- MSE of the relative price differences:

$$MSE = \min_{\Theta} \frac{1}{N} \sum_{n=1}^{N} \frac{(C_n^{market} - C_n^{model}(\Theta))^2}{C_n^{market}}) \tag{26}$$

- MSE of the implied volatility differences:

$$MSE = \min_{\Theta} \frac{1}{N} \sum_{n=1}^{N} (\sigma_n^{\text{market imp}} - \sigma_n^{\text{model imp}}(\Theta))^2 \tag{27}$$

where Θ is the model parameter vector, C_n^{market} and C_n^{model} are the market and model prices of the call option respectively. $\sigma^{\text{market imp}}$ is the market implied volatilities, such gives a BSM option value equal to market price, C^{market}. $\sigma^{\text{model imp}}(\Theta)$ is the model implied volatilities, such gives a BSM option value equal to model price $C^{model}(\Theta)$

In the first stage of our framework, we use the MSE of the price differences, from now called by MSE–prices for short, given by (25), in the calibration. The main reason for choosing the MSE–prices is the fitting process will be quite straightforward. Parameter set Θ in HJM–SV model will be estimated by fitting the model option prices to the market values, just in comparison with MSE of the implied volatility differences, called MSE–impVol for short, which requires a considerable amount of time trying to fetch the implied volatility from the Black–Scholes formula using the scheme which was described in section 2.5.

Furthermore, the implied volatilities are the target of the calibration procedure, so in the second stage of our framework, we use MSE of the implied volatility differences, given by (27), as our error function in calibration.

4.2 Nelder–Mead (Brute–Force) algorithm

While calibrating, we use a Nelder–Mead simplex algorithm [29] to find the minimum of our objective function, which has a set variable Θ. The Nelder–Mead algorithm has a long history of successful use in applications, even though it will usually be slower than an algorithm that uses first or second derivative information. In addition, since there currently is no complete theory describing when the algorithm will successfully converge to the minimum, or how fast it will if it does, for convergence both the ftol and xtol criteria must be met. Thus we decide to set ftol and xtol equal to 0.001 with belief that our function achieves convergence. By doing that we accept the sacrifice in computing time.

4.3 Results

In this subsection, we show the experimental results in our two calibration rounds. The motivation of conducting two separate calibration rounds is given as follows.

The first round of calibration characterized by:

- Data time spans from Jan 2017–Dec 2017
- There are 13 strikes per one maturity in each time to maturity option class. That means, no cleaning data step has been made and this leads to the availability of extremely ITM or OTM options.
- Try with both objective function mention in 4.1

The aim in this round is to compare the calibrated results when using the objective function MSE–prices and MSE–impVol.

The second round of calibration characterized by:

- Use only the MSE–impVol objective function
- Data time spans from Nov 2019–Nov 2020
- There are 8 strikes per one maturity in each time to maturity option class as we add an extra condition while selecting options for calibration. We eliminating those options which are extremely in ITM or OTM by setting the condition for option Selection before calibrating: choose only options, which has $abs(K - S0)/S0 < tol$, where tol is the percent ITM/OTM options, and in our experiment we choose a $tol = 0.02$.

The aim of the second round of calibration is to compare the calibrated results for before and after the market crash in March 2020.

4.3.1 Parameter estimates from calibration with MSE–prices vs MSE–impVol

Using different objective functions in the calibration procedure will definitely lead to different outputs. Each objective function has its own advantages and drawbacks. The motivation for us to use MSE–prices and MSE–impVol have been explained in the previous subsection. Thus in the following, we show how the MSE–impVol works in comparison to MSE–prices in our evaluation.

In order to show the summary results for an arbitrary date in the first round time spans, we select the day 2017/12/11. Table 1 and Table 2 illustrate the comparison errors when calibrated on call options ABB stock on 2017/12/11, using the two different objective functions.

Parameters		kappa	theta	sigma	rho	V_0
Short maturity	MSE prices	1.018	0.297	0.777	-0.090	0.007
	MSE impVol	1.068	0.445	0.975	-0.060	0.000
Medium maturity	MSE prices	1.953	0.013	0.047	-1.000	0.025
	MSE impVol	0.961	0.012	0.151	-0.652	0.024
Long maturity	MSE prices	13.522	0.020	0.359	-1.000	0.055
	MSE impVol	0.084	0.020	0.047	-0.994	0.023

Table 1: Comparison calibrated parameters using different objective functions. Calibrated on call options ABB stock on 2017/12/11.

Figure 3a illustrates the comparison between ABB stock calls model values and market values. Figure 3b illustrates the comparison between ABB stock calls model

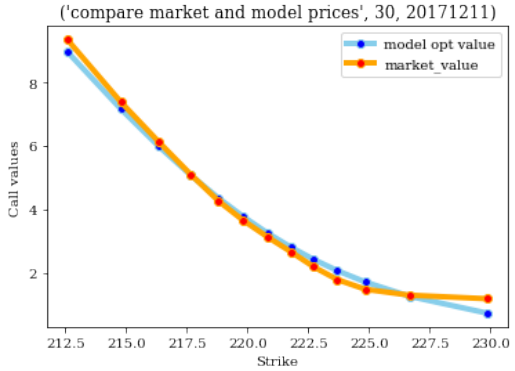

(a) Compare market with model option premiums ABB calls on 2017/12/11; for maturity class $T_1 = 30$ days.

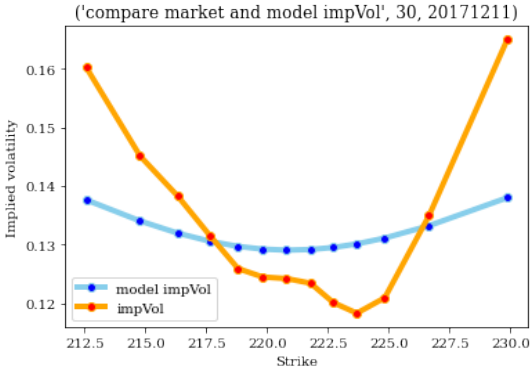

(b) Compare market with model option impVol ABB calls on 2017/12/11; for maturity class $T_1 = 30$ days.

Figure 3: Compare market with model result on ABB calls on 2017/12/11.

impVol and market impVol. Obviously, the model impVol is far from fit to market imVol curve. Thus, one conclusion can be made is that using the MSE–prices objective function, the calibrated results lead to a well-fitted model call values to market call values while does not perform well on the target of the optimization which is generating a similar smile curve as market impVol.

We show on Figure 4 the comparison between market impVol and model impVol for medium maturity class of ABB options, which have 60 days $\leq T_2 \leq$ 182 days. While Figure 5 the comparison–for the long maturity class, 273 days $\leq T_3 \leq$ 730 days. From these comparisons, we can see that the HJM–SV model still works for medium maturity class, but does not capture well the long maturity class. For the long maturity class options, the model impVol curves loose the form of smiles/skews. They are displayed as linear lines with negative slopes, which are significant different from the market impVol curves.

In addition to visualize comparison the , we would like to use the numerical comparison in order to have a fair evaluate on which objective function works better for our calibration. Thus we use the mean absolute error (MAE), as shown in the Table 2, between market and model impVol. The MAE is calculated as follows:

$$MAE = \frac{1}{13}\sum_{i=1}^{N}|(\sigma_i^{\text{market}} - \sigma_i^{\text{model}})|$$

where i is the i^{th} option in the 13 options used for calibration on 2017/12/11.

From Table 2, one can see that the MSE–impVol gives us smaller MAEs value in all maturity class calibration. Therefore, from now on we focus on displaying experimental results of calibration using MSE–impVol. This is also the main reason that in the next section, while calibrating with new data time spans we only apply

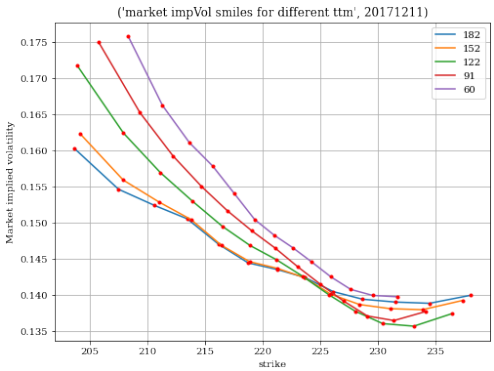

(a) Market ImpVol smiles for different maturities

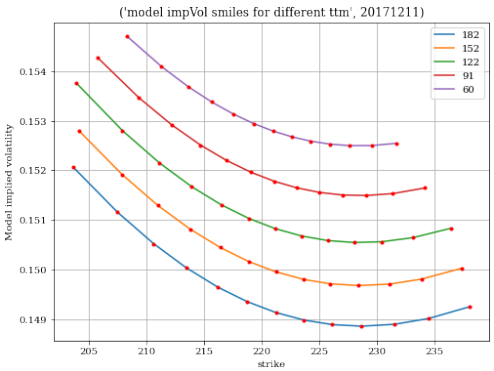

(b) Model ImpVol smiles for different maturities

Figure 4: Compare market with model result on ABB calls on 2017/12/11.Medium maturity class 60 days $\leq T_2 \leq$ 182 days, ABB stock call options

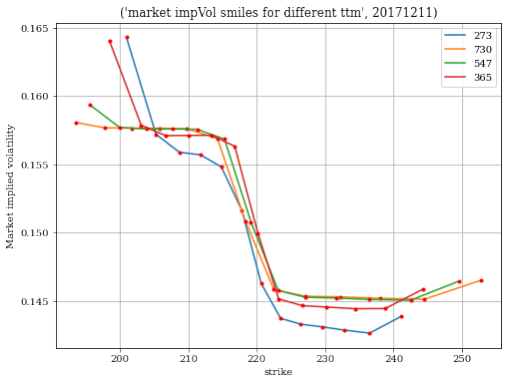

(a) Market ImpVol smiles for different maturities

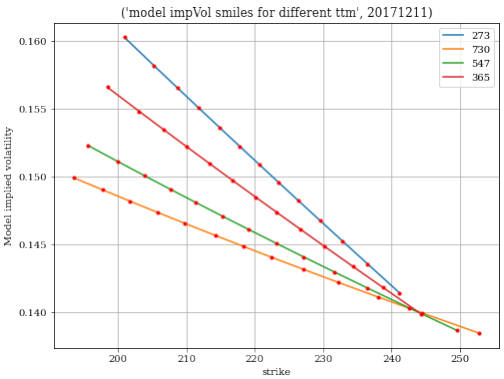

(b) Model ImpVol smiles for different maturities

Figure 5: Compare market with model result on ABB calls on 2017/12/11. Long maturity class 273 days $\leq T_3 \leq$ 730 days, ABB stock call options

MSE–impVol as our objective function. Besides, the HJM–SV model does not capture well the long maturity class, we, therefore, eliminate the long maturity in the second round of calibration with data time spans from Dec 2019–Dec 2020.

Parameter		MAE
Short Maturity Class	MSE prices	0.0093
	MSE impVol	0.0088
Medium Maturity class	MSE prices	0.0056
	MSE impVol	0.0038
Long Maturity class	MSE prices	0.00466
	MSE impVol	0.0030

Table 2: MAE between market and model implied volatility for different maturity classes and with different choices of objective function, on 2017/12/11.

In the attempt of investigating whether or not the calibrated parameters on a trading day could be useful in forecasting the impVol of the options in the near future, we use the calibrated parameter set of a day, and apply it the day after, i.e. *the next trading day*. Then we evaluate the error that it generates. We call this error as *the next day error*. Table 3 shows the next day errors for each maturity class on the trading date 2017/12/12.

Parameter	MAE
Short Maturity Class	0.009
Medium Maturity class	0.0085
Long Maturity class	0.00363

Table 3: Using calibrated parameters on 2017/12/11 to calculate the model impVol in the next trading day, 2017/12/12.

4.3.2 Parameter estimates for data before vs after Covid 19

Figure 6 and Figure 7 show the resulting model values compared to the market quotes of the ABB stock call options and EX50 call options, respectively. Although this is not the direct target of the optimization, the calibrated parameters set gives us quite fitted model values to its market values.

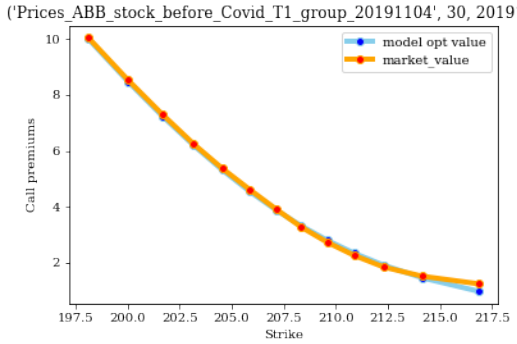

(a) Compare market and model option premiums of EX50 calls on 2019/11/04; for maturity class $T_1 = 30$ days.

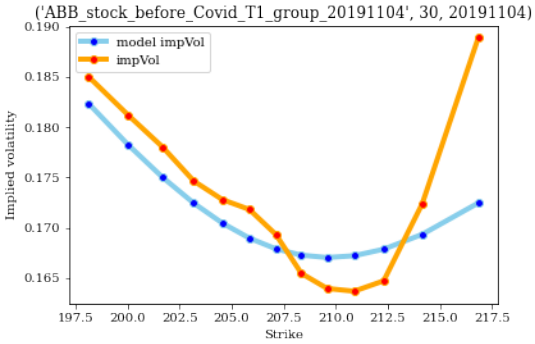

(b) Compare model impVol and market imp Vol of ABB calls on 2019/11/04; for maturity class $T_1 = 30$ days.

Figure 6: Compare calibrated results on ABB stock calls on 2019/11/04; for maturity class $T_1 = 30$ days.

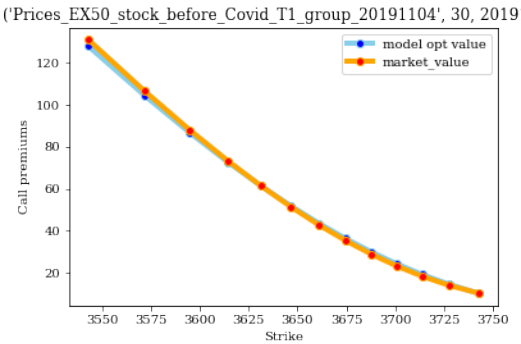

(a) Compare market and model option premiums of EX50 calls on 2019/11/04; for maturity class $T_1 = 30$ days.

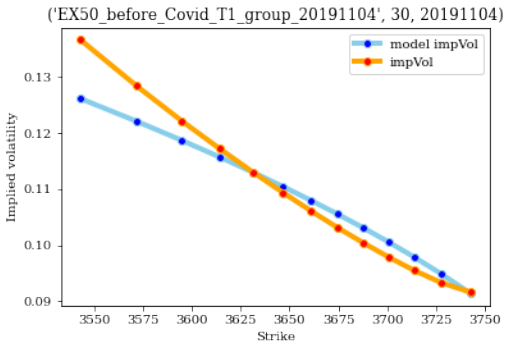

(b) Compare model impVol and market imp Vol of EX50 calls on 2019/11/04; for maturity class $T_1 = 30$ days.

Figure 7: Compare calibrated results on EX50 calls on 2019/11/04; for maturity class $T_1 = 30$ days.

Figure 8 show the resulting model impVols compared to the market impVols. We want to recall that we used the error function (27) used in our calibration.

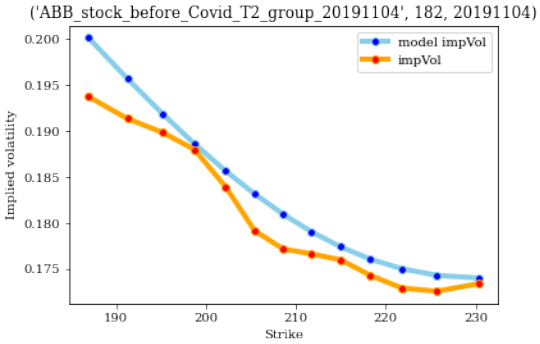

(a) Compare model impVol and market imp Vol of ABB calls on 2019/11/04

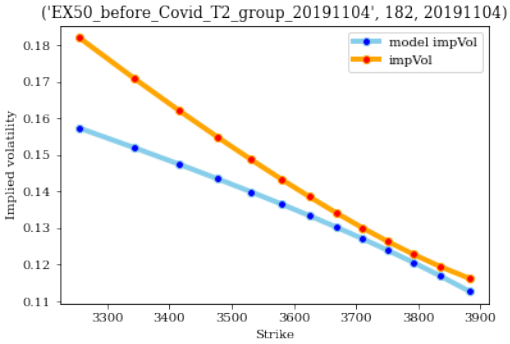

(b) Compare model impVol and market imp Vol of EX50 calls on 2019/11/04

Figure 9: Compare market with model results on 2019/11/04; for maturity class 60 days $\leq T_2 \leq$ 182 days.

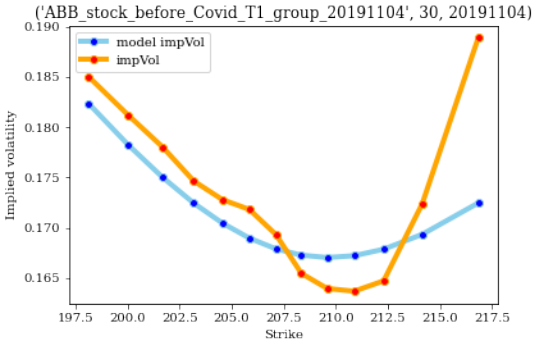

(a) Compare model impVol and market imp Vol of ABB calls on 2019/11/04; for maturity class $T_1 = 30$ days.

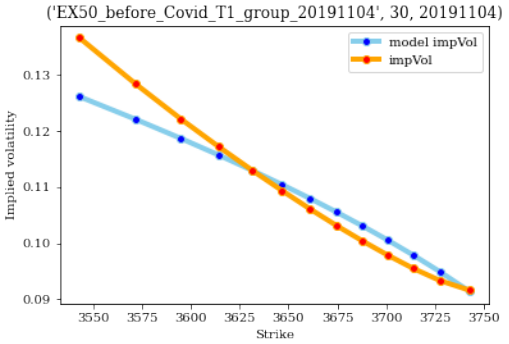

(b) Compare model impVol and market impVol of EX50 calls on 2019/11/04; for maturity class $T_1 = 30$ days.

Figure 8: Compare model impVol and market impVol. Short maturity class $T_1 = 30$ days.

Similarly, we generate the plots to compare HJM–SV model impVol and market imp Vol for the medium group maturity 60 days $\leq T_2 \leq$ 182 days. The plots for ABB stock and EX50 are respectively Figure 9a, and Figure 9b.

In the appendix B.1, we illustrate the daily MAE of the market and HJM–SV model impVol of ABB calls in Jan 2020, Feb 2020, Mar 2020, and Apr 2020. The last column shows how well the estimates for parameters set Θ in HJM–SV model work on the next trading days in term of forecasting the volatility.

The MAE calibrated with ABB stock, and EX50 call options for short maturity class (= 30 days) are shown in the following Table 4. From this table one can see that the errors in period before the pandemic is relatively smaller than the error in the crisis month of the pandemic, e.g. Mar 2020 and Apr 2020. A reasonable explanation could be that our input ranges for initial parameter guesses are unchanged in the

calibrations for the most and the least market fluctuated days. As a result, it would be hard to have a good approximation of optimal parameter set.

Calibration with MSE–impVol	Average of MAE for daily calibration			
	Before Covid		After Covid	
	Jan 2020	Feb 2020	Mar 2020	Apr 2020
Short maturity, ABB stock	0.0013	0.0014	0.0433	0.0350
Short maturity, EUROSTOX50 index	0.0001	0.00006	0.1590	0.000001

Table 4: Compare errors when calibrating with MSE–impVol before and after the Covid pandemic.

5 Conclusions

In our work, we use a large data set on daily implied volatility surfaces to calibrate our proposed HJM–SV model, and from the experimental results we observe that the new model works better for the maturity classes less than 6 months, rather than the long maturity from 9 months up to 2 years. In particular, the model adequately fits observed short maturity option class (30 days) and medium maturity maturity option class (from 60 days up to 180 days) in the period from Jan 2017 to Dec 2017 and from Nov 2019 to Nov 2020, while it fails on the long maturity class (from 273 days to 730 days) in the same time period.

Besides, a combination of the expected speed and ease of implementation made us go with a choice of using Fourier–based approach option pricing in our work. We believe that applying the Fourier–based method could allow us to expand the work in the future for using HJM–SV model in different designed markets. It means once the framework is set up, other different S_t-models can be evaluated simply by interchanging the characteristic equations. The calculations in this method could be done quickly and with good accuracy, while the surfaces produced should have neat shapes.

Future works

As reported in the calibrated results section, for the long maturity class from 273 days up to 730 days, we could not find reasonable estimates of parameter set in HJM–SV. Perhaps we need to include more constraints in the model in order to build a implied volatility curve for options maturity class above 1 year. As mentioned in the section 2.1.4, some researchers including Y. Le Cam and S. Galluccio, have claimed that SV–jump diffusion models matches the market better than the use SV types alone. One potential approach to improve our HJM–SV model is adding the jump confusion process to the SV of underlying asset prices.

References

[1] Chang Ahn and Howard Thompson. An analysis of some aspects of regulatory risk and the required rate of return for public utilities. *Journal of Regulatory Economics*, 1:241–257, 09 1989.

[2] Elie Ayache. *The Blank Swan: The End of Probability*. Wiley, 2010.

[3] Gurdip Bakshi, Charles Cao, and Zhiwu Chen. Empirical performance of alternative option pricing models. *The Journal of Finance*, 52(5):2003–2049, 1997.

[4] David S. Bates. Post-87 crash fears in the S&P 500 futures option market. *Journal of Econometrics*, 94(1):181–238, 2000.

[5] Fischer Black and Myron Scholes. The pricing of options and corporate liabilities. *Journal of Political Economy*, 81(3):637–654, 1973.

[6] Menachem Brenner and Marti Subrahmanyam. A simple formula to compute the implied standard deviation. *Financial Analysts Journal*, 44:80–83, 09 1988.

[7] Damiano Brigo and Fabio Mercurio. *The Heath-Jarrow-Morton (HJM) Framework*, pages 173–182. Springer Berlin Heidelberg, Berlin, Heidelberg, 2001.

[8] Mikhail Chernov and Eric Ghysels. A study toward a unified approach to the joint estimation of objective and risk neutral measures for the purpose of options valuation. *Journal of Financial Economics*, 56:407–458, 06 2000.

[9] Peter Christoffersen, Steven Heston, and Kris Jacobs. The shape and term structure of the index option smirk: Why multifactor stochastic volatility models work so well. *Management Science*, 55(12):1914–1932, 2009.

[10] John C. Cox, Jonathan E. Ingersoll, and Stephen A. Ross. A theory of the term structure of interest rates. *Econometrica*, 53(2):385–407, 1985.

[11] Yahoo Finance. Market quotes indices. `https://finance.yahoo.com/`. Accessed: 2021-05-26.

[12] Stefano Galluccio and Yann Lecam. Implied calibration and moments asymptotics in stochastic volatility jump diffusion models. *SSRN Electronic Journal*, 04 2008.

[13] J. Gatheral and N.N. Taleb. *The Volatility Surface: A Practitioner's Guide*. Wiley Finance. Wiley, 2006.

[14] Jim Gatheral. Consistent modeling of S&P 500 and VIX options. 01 2008.

[15] ABB Group. Abb group. `https://global.abb/group/en`, 2021.

[16] David Heath, Robert Jarrow, and Andrew Morton. Bond Pricing and the Term Structure of Interest Rates: A New Methodology for Contingent Claims Valuation. *Econometrica*, 60(1):77–105, January 1992.

[17] Steven L Heston. A closed-form solution for options with stochastic volatility with applications to bond and currency options. *Review of Financial Studies*, 6(2):327–43, 1993.

[18] Y. Hilpisch. *Derivatives Analytics with Python: Data Analysis, Models, Simulation, Calibration and Hedging*. EBL-Schweitzer. Wiley, 2015.

[19] John C Hull. *Options, Futures and Other Derivatives*. Pearson Education Asia, New Delhi, 6 edition, 2003. Futures and Options(332.6452).

[20] SX5E Index. Sx5e index. `https://www.bloomberg.com/quote/SX5E:IND`, 2021.

[21] Christopher Jones. The dynamics of stochastic volatility: Evidence from underlying and options markets. *Journal of Econometrics*, 116:181–224, 09 2003.

[22] Joerg Kienitz and Daniel Wetterau. *Financial Modelling : Theory, Implementation and Practice with MATLAB Source*. John Wiley & Sons, 2018.

[23] Alan Lewis. A simple option formula for general jump- diffusion and other exponential lévy processes. *Envision Financial Systems and OptionCity.net*, 2001.

[24] OptionMetrics LLC. Data Products option metrics description. `https://optionmetrics.com/data-products/`. Accessed: 2021-05-21.

[25] Benoît Mandelbrot. The variation of certain speculative prices. *The Journal of Business*, 36:394–419, 1963.

[26] Angelo Melino and Stuart M. Turnbull. Pricing foreign currency options with stochastic volatility. *Journal of Econometrics*, 45(1):239–265, 1990.

[27] Robert Merton. Option prices when underlying stock returns are discontinuous. *Journal of Financial Economics*, 3:125–144, 01 1976.

[28] Saikat Nandi. How important is the correlation between returns and volatility in a stochastic volatility model? empirical evidence from pricing and hedging in the S&P 500 index options market. *Journal of Banking & Finance*, 22(5):589–610, 1998.

[29] J. Nelder and R. Mead. Errata. *The Computer Journal*, 8(1):27–27, 04 1965.

[30] R. R. Officer. The variability of the market factor of the new york stock exchange. *The Journal of Business*, 46(3):434–453, 1973.

[31] Jun Pan. The jump-risk premia implicit in options: evidence from an integrated time-series study. *Journal of Financial Economics*, 63(1):3–50, 2002.

[32] Andrea Pascucci and Agliardi R. *PDE and Martingale Methods in Option Pricing*, pages 429 – 495. 01 2011.

[33] Jan R. M. Roman. *Analytical Finance: Volume I - The Mathematics of Equity Derivatives, Markets, Risk and Valuation.* Palgrave Macmillan, 2017.

[34] J.R.M. Röman. *Analytical Finance: Volume II: The Mathematics of Interest Rate Derivatives, Markets, Risk and Valuation.* Springer International Publishing, 2017.

[35] Y. Le Cam S. Galluccio. Implied Calibration and Moments Asymptotics in Stochastic Volatility Jump Diffusion Models. *Probability and Financial Mathemat- ics team, Evry University*, 60(1):251, 2007.

[36] Elias M. Stein and Jeremy C. Stein. Stock price distributions with stochastic volatility: An analytic approach. *Review of Financial Studies*, 4:727–752, 1991.

[37] María Suárez-Taboada, Jeroen A. S. Witteveen, Lech A. Grzelak, and Cornelis W. Oosterlee. Uncertainty quantification and heston model. *Journal of Mathematics in Industry*, 8(1):5, 05 2018.

A Appendix Sample Data

A.1 ABB call option data

	Date	Tau	impVol	strike	spot
0	20191101	30	0.179552	211.9350	202.69
1	20191101	30	0.164527	209.4650	202.69
2	20191101	30	0.159766	207.8251	202.69
3	20191101	30	0.159766	206.5054	202.69
4	20191101	30	0.160149	205.2670	202.69
...	...	...	...	...	...
2725	20191129	730	0.186581	198.7806	209.47
2726	20191129	730	0.192117	193.2670	209.47
2727	20191129	730	0.194116	188.2893	209.47
2728	20191129	730	0.194365	183.1361	209.47
2729	20191129	730	0.194473	178.0555	209.47

2730 rows × 5 columns

Figure 10: Snapshoot of calls on ABB stock in Nov 2019 from IvyDBEurope

	Date	Tau	impVol	strike	spot	r	market_value
3	20191101	30	0.159766	206.5054	202.69	0.0	2.159966
4	20191101	30	0.160149	205.2670	202.69	0.0	2.612809
5	20191101	30	0.160631	204.0715	202.69	0.0	3.111531
6	20191101	30	0.162212	202.8979	202.69	0.0	3.685023
7	20191101	30	0.164508	201.7050	202.69	0.0	4.343001
...	...	...	...	...	...	...	...
2685	20191129	273	0.182033	207.1176	209.47	0.0	14.368221
2697	20191129	365	0.183664	210.0586	209.47	0.0	15.161533
2698	20191129	365	0.183874	206.1540	209.47	0.0	17.042435
2710	20191129	547	0.184007	209.3416	209.47	0.0	18.972310
2723	20191129	730	0.184045	208.6500	209.47	0.0	22.208308

603 rows × 7 columns

Figure 11: Snapshoot of one sample data of calls on ABB stock used in calibration

A.2 EURO STOXX 50 call option data

	Date	Tau	impVol	strike	spot
0	20191101	30	0.091724	3700.216	3620.0
1	20191101	30	0.093577	3685.352	3620.0
2	20191101	30	0.095772	3671.806	3620.0
3	20191101	30	0.098200	3658.851	3620.0
4	20191101	30	0.100827	3646.042	3620.0
...	...	...	...	...	...
2725	20191129	730	0.165848	3283.811	3693.0
2726	20191129	730	0.172145	3166.306	3693.0
2727	20191129	730	0.179797	3034.262	3693.0
2728	20191129	730	0.189149	2880.441	3693.0
2729	20191129	730	0.200147	2694.651	3693.0

2730 rows × 5 columns

Figure 12: Snapshoot of calls on Eurostoxx 50 in Nov 2019 from IvyDBEurope

	Date	Tau	impVol	strike	spot	r	market_value
0	20191101	30	0.091724	3700.216	3620.0	0.0	11.089797
1	20191101	30	0.093577	3685.352	3620.0	0.0	15.017913
2	20191101	30	0.095772	3671.806	3620.0	0.0	19.505371
3	20191101	30	0.098200	3658.851	3620.0	0.0	24.616096
4	20191101	30	0.100827	3646.042	3620.0	0.0	30.436017
...	...	...	...	...	...	...	...

Figure 13: Snapshoot of one sample data of calls on Eurostoxx 50 used in calibration

A.3 Supporting figures

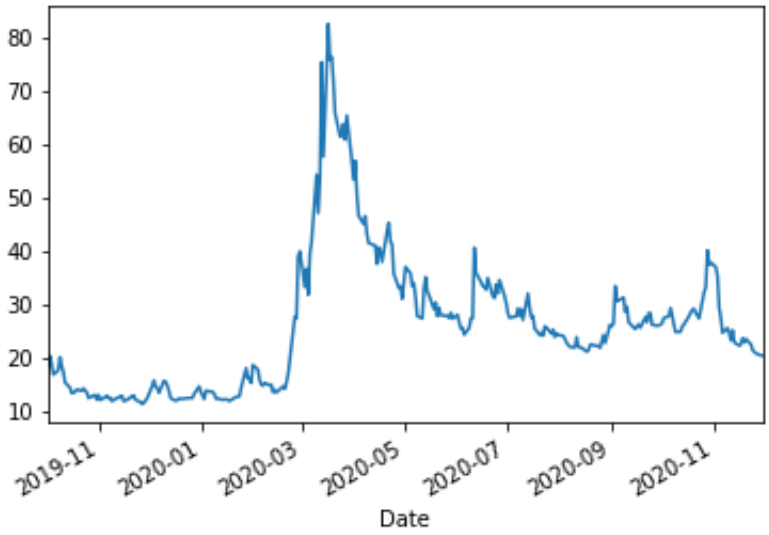

Figure 14: CBOE Volatility Index (VIX) index from Jan 01, 2019 to Nov 30, 2020; currency in USD

B Appendix Results

B.1 Mean absolute error between model and market impVol– calibrated on ABB options data

	date	error	next_date	next_error
0	20200102	-0.000302	20200103	0.001189
1	20200103	-0.000064	20200107	0.012593
2	20200107	-0.001847	20200108	-0.001982
3	20200108	-0.003196	20200109	0.003799
4	20200109	0.001088	20200110	0.009061
5	20200110	-0.002065	20200113	0.007401
6	20200113	-0.000552	20200114	-0.005300
7	20200114	-0.000651	20200115	0.010333
8	20200115	-0.002971	20200116	-0.034152
9	20200116	-0.001243	20200117	0.019383
10	20200117	0.001312	20200120	0.001530
11	20200120	0.001748	20200121	-0.008177
12	20200121	0.001492	20200122	0.000812
13	20200122	0.002389	20200123	0.013250
14	20200123	-0.001893	20200124	-0.026709
15	20200124	0.001770	20200127	0.055753
16	20200127	0.004082	20200128	-0.020545
17	20200128	0.000220	20200129	-0.015817
18	20200129	-0.002856	20200130	0.001088
19	20200130	-0.000759	20200131	0.009988

Figure 15: ABB calls data; Mean absolute error between model and market impVol in Jan 2020

	date	error	next_date	next_error
0	20200203	0.000585	20200204	0.001337
1	20200204	-0.000929	20200205	-0.055464
2	20200205	-0.000426	20200206	0.013790
3	20200206	0.001152	20200207	0.005443
4	20200207	-0.001125	20200210	-0.010050
5	20200210	-0.000273	20200211	-0.002264
6	20200211	-0.002119	20200212	-0.001328
7	20200212	-0.000573	20200213	0.002098
8	20200213	-0.001121	20200214	0.000785
9	20200214	-0.001237	20200217	-0.010009
10	20200217	-0.004880	20200218	-0.009940
11	20200218	-0.000522	20200219	-0.000083
12	20200219	-0.000584	20200220	0.032157
13	20200220	-0.000587	20200221	0.005661
14	20200221	0.003095	20200224	0.061583
15	20200224	0.001721	20200225	-0.007976
16	20200225	-0.003767	20200226	-0.051090
17	20200226	-0.006963	20200227	0.071178
18	20200227	-0.008180	20200228	0.044716

Figure 16: ABB calls data; Mean absolute error between model and market impVol in Feb 2020

	date	error	next_date	next_error
0	20200302	-0.008471	20200303	-0.042601
1	20200303	-0.007280	20200304	-0.055813
2	20200304	-0.003623	20200305	0.045232
3	20200305	0.002118	20200306	0.096953
4	20200306	-0.002239	20200309	0.216467
5	20200309	0.001839	20200310	-0.038667
6	20200310	-0.001482	20200311	-0.002432
7	20200311	0.006628	20200312	0.289097
8	20200312	-0.096015	20200313	-0.071574
9	20200313	0.009423	20200316	0.223939
10	20200316	-0.112543	20200317	-0.415806
11	20200317	-0.113432	20200318	-0.055317
12	20200318	-0.117505	20200319	0.031127
13	20200319	-0.053716	20200320	-0.390979
14	20200320	-0.156768	20200323	0.329640
15	20200323	-0.059569	20200324	-0.383933
16	20200324	-0.002473	20200325	0.186886
17	20200325	-0.188281	20200326	-0.620222
18	20200326	-0.021496	20200327	0.177565
19	20200327	0.010601	20200330	-0.271192
20	20200330	0.004972	20200331	-0.070090

Figure 17: ABB calls data; Mean absolute error between model and market impVol in Mar 2020

	date	error	next_date	next_error
0	20200401	-0.003783	20200402	-0.046919
1	20200402	-0.005165	20200403	-0.041864
2	20200403	-0.008086	20200406	-0.004502
3	20200406	0.002114	20200407	0.005233
4	20200407	-0.027373	20200408	-0.011116
5	20200408	-0.002440	20200409	-0.009038
6	20200409	0.000029	20200414	-0.019064
7	20200414	-0.006425	20200415	0.053654
8	20200415	0.007870	20200416	0.011194
9	20200416	-0.004427	20200417	-0.047531
10	20200417	0.005962	20200420	-0.083870
11	20200420	-0.027687	20200421	0.100200
12	20200421	-0.007802	20200422	-0.011075
13	20200422	0.004879	20200423	-0.060959
14	20200423	-0.013553	20200424	-0.031437
15	20200424	0.000070	20200427	-0.056577
16	20200427	-0.007503	20200428	-0.057206
17	20200428	0.001373	20200429	-0.003554
18	20200429	-0.003400	20200430	0.030316

Figure 18: ABB calls data; Mean absolute error between model and market impVol in Apr 2020

	date	error	next_date	next_error
0	20200102	0.000099	20200103	0.017593
1	20200103	-0.000160	20200106	0.007057
2	20200106	0.000669	20200107	-0.001410
3	20200107	0.000923	20200108	-0.005044
4	20200108	0.001407	20200109	-0.005780
5	20200109	0.000956	20200110	-0.001610
6	20200110	-0.001892	20200113	-0.003135
7	20200113	0.002179	20200114	0.000426
8	20200114	0.000204	20200115	0.000335
9	20200115	-0.001198	20200116	-0.007741
10	20200116	0.000159	20200117	-0.003009
11	20200117	-0.000929	20200120	0.002623
12	20200120	-0.001975	20200121	0.005192
13	20200121	0.001406	20200122	0.005301
14	20200122	-0.000326	20200123	0.001847
15	20200123	0.000148	20200124	0.002907
16	20200124	0.000315	20200127	0.038235
17	20200127	0.000878	20200128	-0.018577
18	20200128	-0.001595	20200129	-0.005900
19	20200129	0.001298	20200130	0.011042
20	20200130	-0.000103	20200131	0.031037

Figure 19: EUROSTOX50 calls data; Mean absolute error between model and market impVol in Jan 2020

	date	error	next_date	next_error
0	20200203	-0.000922	20200204	-0.022750
1	20200204	-0.000988	20200205	-0.013559
2	20200205	-0.000615	20200206	-0.005555
3	20200206	0.002045	20200207	0.008117
4	20200207	0.000104	20200210	-0.000407
5	20200210	0.001368	20200211	0.002526
6	20200211	-0.000770	20200212	-0.011708
7	20200212	-0.002202	20200213	0.005834
8	20200213	0.000877	20200214	0.000514
9	20200214	0.000453	20200217	0.000013
10	20200217	-0.000159	20200218	0.006084
11	20200218	0.000916	20200219	-0.005370
12	20200219	0.001529	20200220	0.036820
13	20200220	-0.001404	20200221	-0.013524
14	20200221	-0.000398	20200224	0.069151
15	20200224	-0.000578	20200225	0.047638
16	20200225	-0.000279	20200226	-0.033404
17	20200226	-0.000420	20200227	0.087471
18	20200227	0.000139	20200228	0.038748

Figure 20: EUROSTOX50 calls data; Mean absolute error between model and market impVol in Feb 2020

	date	error	next_date	next_error
0	20200302	-0.000604	20200303	0.005314
1	20200303	0.000168	20200304	-0.062270
2	20200304	0.000815	20200305	0.074358
3	20200305	-0.000343	20200306	0.064141
4	20200306	0.000315	20200309	0.197888
5	20200309	-0.000251	20200310	-0.122382
6	20200310	0.000105	20200311	0.060147
7	20200311	0.000044	20200312	0.206808
8	20200312	0.622323	20200313	0.538970
9	20200313	0.000003	20200316	0.171004
10	20200316	0.712975	20200317	0.593072
11	20200317	0.593072	20200318	0.657652
12	20200318	0.657652	20200319	0.595563
13	20200319	0.595563	20200323	0.491971
14	20200323	0.000198	20200324	-0.107479
15	20200324	-0.000032	20200325	0.041906
16	20200325	-0.000177	20200326	-0.030157
17	20200326	-0.000255	20200327	0.072521
18	20200327	-0.000086	20200330	-0.056095
19	20200330	-0.000014	20200331	-0.048771

Figure 21: EUROSTOX50 calls data; Mean absolute error between model and market impVol in Mar 2020

	date	error	next_date	next_error
0	20200401	0.000272	20200402	-0.031464
1	20200402	-0.000079	20200403	-0.026185
2	20200403	0.000217	20200406	-0.052764
3	20200406	0.000301	20200407	0.047817
4	20200407	-0.000048	20200408	-0.030994
5	20200408	0.000086	20200409	-0.001669
6	20200409	0.000261	20200414	-0.031506
7	20200414	0.000262	20200415	0.044317
8	20200415	-0.000317	20200416	-0.015444
9	20200416	0.000179	20200417	-0.030726
10	20200417	-0.000135	20200420	0.020569
11	20200420	0.000090	20200421	0.050733
12	20200421	-0.000164	20200422	-0.036430
13	20200422	0.000188	20200423	-0.011942
14	20200423	0.000070	20200424	-0.029151
15	20200424	-0.000296	20200427	-0.045917
16	20200427	-0.000093	20200428	-0.005952
17	20200428	-0.000154	20200429	-0.031750
18	20200429	-0.000617	20200430	0.034658

Figure 22: EUROSTOX50 calls data; Mean absolute error between model and market impVol in Apr 2020